Energy Uptake and Allocation During Ontogeny

Chen Hou,[1]* Wenyun Zuo,[2] Melanie E. Moses,[3] William H. Woodruff,[1,4] James H. Brown,[1,2] Geoffrey B. West[1,4]

All organisms face the problem of how to fuel ontogenetic growth. We present a model, empirically grounded in data from birds and mammals, that correctly predicts how growing animals allocate food energy between synthesis of new biomass and maintenance of existing biomass. Previous energy budget models have typically had their bases in rates of either food consumption or metabolic energy expenditure. Our model provides a framework that reconciles these two approaches and highlights the fundamental principles that determine rates of food assimilation and rates of energy allocation to maintenance, biosynthesis, activity, and storage. The model predicts that growth and assimilation rates for all animals should cluster closely around two universal curves. Data for mammals and birds of diverse body sizes and taxa support these predictions.

The "food of life" and the "fire of life"—the combustion of food to supply the energy that fuels growth, maintenance, and activity—is fundamental to animal survival (*1*). A large body of previous work used energy budget models to understand ontogenetic growth (*1*–*7*). These models have contributed importantly to many conceptual and applied problems, including life history theory, animal husbandry, and biomedicine. Still largely missing, however, is a complete quantitative framework that specifies how food is transformed into metabolic energy and stored biomass. Here, we present such a framework, which quantifies explicitly how assimilated food is transformed into biomass and metabolic energy during ontogeny.

When an animal is growing, some fraction of the assimilated food is oxidized to fuel the total metabolic rate, B_{tot}, whereas the remaining fraction is synthesized and stored as biomass, S (Fig. 1). Thus, the energy flux of assimilated food, A, sometimes called the rate of intake of metabolizable energy (*1*, *2*), is expressed as

$$A = B_{tot} + S = B_{tot} + E_c\, dm/dt \qquad (1)$$

where A is defined as the combustion energy content of ingested food per unit time minus the combustion energy content of excreta per unit time, E_c is the combustion energy content of a unit biomass, and dm/dt is the rate of change in biomass, m, at time, t.

We build on an ontogenetic growth model (OGM), which specifies the allocation of metabolic energy between growth and maintenance and views the scaling of metabolic rate with body size as the primary constraint on growth (*7*). It partitions the basal metabolic rate, B_{basal}, between the rate of energy expenditure to maintain the existing biomass, B_{maint}, and the rate to synthesize the new biomass, B_{syn} (Fig. 1): so, $B_{basal} = B_{maint} + B_{syn} = B_m m + E_m dm/dt$, where $B_m \sim M^{-1/4}$ is the mass-specific maintenance metabolic rate, M is the adult body mass, and E_m is the energy required to synthesize a unit of biomass.

It is difficult to measure B_{basal} over ontogeny because animals grow even while resting. Therefore, for growing animals a more operational and realistic parameter is resting metabolic rate, B_{rest}, which is the sum of B_{basal} and specific dynamic action (SDA), the increment resulting from digestion. SDA is the energy expended for intestinal absorption, nutrient transport, amino acid oxidation, and protein synthesis (*8*, *9*). Because some fraction of metabolic rate is allocated to SDA during growth (*8*–*11*), we modify the OGM to obtain

$$B_{rest} = B_{maint} + B_{syn} = B_m m + E_m dm/dt \qquad (2)$$

where B_m is larger here than in the OGM, which ignored SDA.

It is important to recognize the difference between the terms $S = E_c dm/dt$ in Eq. 1 and $B_{syn} = E_m dm/dt$ in Eq. 2 and, consequently, the difference between E_m and E_c. Energy expended during growth is partitioned between the energy content stored in the newly synthesized biomass and the energy expended in synthesizing this biomass from the constituent materials. So, S is the rate of accumulated energy content of new biomass, and E_c is its combustion energy content. On the other hand, B_{syn} is the metabolic power expended on biosynthesis, and E_m is the energy expended to synthesize a unit of biomass. The term B_{syn} corresponds to the organizational work of growth (*2*) and is completely dissipated as heat, not conserved in stored biomass. In the OGM, the energy expended on biosynthesis was incorrectly estimated by using the empirical combustion energy (*7*).

For adult mammals and birds, the total metabolic rate is typically referred to as field metabolic rate, and the relationship between total and resting metabolic rates is expressed as $B_{tot}(M) = B_{act}(M) + B_{rest}(M) = fB_{rest}(M)$, where B_{act} is the rate of energy expenditure for locomotion, feeding, and other activities and f, the activity scope, is a dimensionless parameter (*12*–*14*). In adult endotherms, f is about 2 to 3 and independent of body mass (*12*–*14*). Assuming that a similar relationship holds during growth, we can write, using Eq. 2, $B_{tot}(m) = fB_{maint}(m) + fB_{syn}(m)$. We define the dimensionless storage coefficient, $\gamma = S/B_{syn} = E_c/E_m$, as the ratio of the energy stored in a unit of biomass to the energy expended to synthesize this biomass. Substituting γ and B_{tot} into Eqs. 1 and 2 gives

$$A(m) = B_{maint}(m) + B_{act}(m) + B_{syn}(m) + S(m)$$
$$= (f + \gamma)B_{rest}(m) - \gamma B_{maint}(m) \qquad (3)$$

Equation 3 is quite general, independent of how B_{rest}, B_{maint}, or f scale with m. Empirical measurements of metabolic rate over ontogeny and theoretical evidence linking growth and metabolism show that resting metabolic rate $B_{rest}(m) \approx B_0 m^{3/4}$ over ontogeny, where B_0 is constant for a given taxon (*14*, *15*). The mass-specific maintenance rate, taking into account SDA, is $B_m \approx$

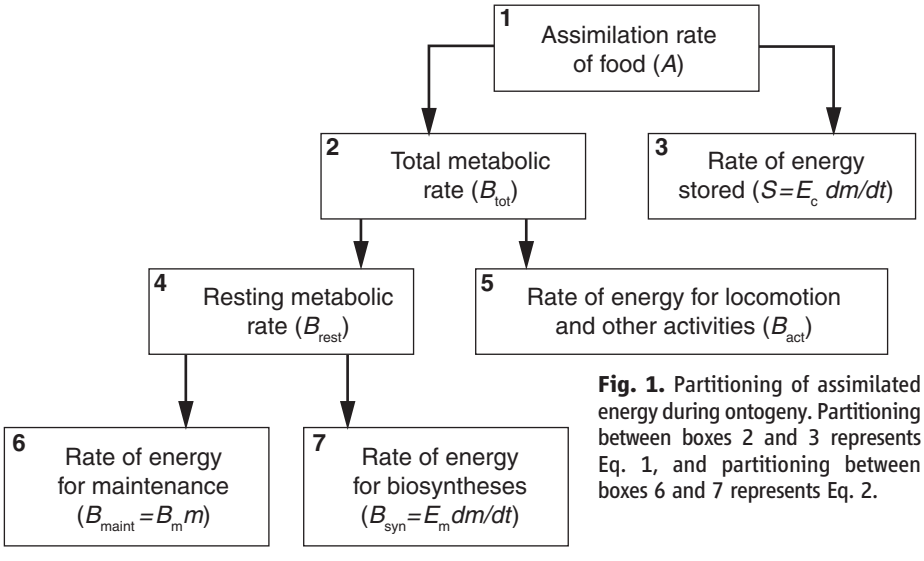

Fig. 1. Partitioning of assimilated energy during ontogeny. Partitioning between boxes 2 and 3 represents Eq. 1, and partitioning between boxes 6 and 7 represents Eq. 2.

[1]Santa Fe Institute, 1399 Hyde Park Road, Santa Fe, NM 87501, USA. [2]Department of Biology, University of New Mexico, Albuquerque, NM 87131, USA. [3]Department of Computer Science, University of New Mexico, Albuquerque, NM 87131, USA. [4]Los Alamos National Laboratory, Los Alamos, NM 87545, USA.

*To whom correspondence should be addressed. E-mail: houc@santafe.edu

$B_0M^{-1/4}$ (*7*). The use of these scaling relations in Eq. 3 yields

$$A(m) = (f+\gamma)B_0m^{3/4} - \gamma B_0M^{-1/4}m$$
$$= B_{\text{rest,adult}}[(f+\gamma)\mu^{3/4} - \gamma\mu] \quad (4)$$

where μ ($\equiv m/M$) is relative mass and $B_{\text{rest,adult}} \approx B_0M^{3/4}$ is the resting metabolic rate at the adult size.

Note that Eq. 4 predicts that during ontogeny the food assimilation rate, A, unlike metabolic rate, does not obey a simple power law as a function of body mass, m. This prediction is well supported (*14*). In Fig. 2, we plot some examples of the normalized assimilation rate ($A/B_{\text{rest,adult}}$) versus μ for six different animals and fit the data with Eq. 4. Values of f, γ, and R^2 from the nonlinear least squares regression for these and several other bird and mammal species are in table S1 (*14*). The storage coefficient, $\gamma = E_c/E_m$, can in principle be determined independently from the energetics of biosynthesis. The energy content of biomass, E_c, averages about 24,000 J/g for dry mass (*16*), with fourfold variation across vertebrates of different taxa and ontogenetic stages (*17*). In contrast to E_c, E_m, the energy expended to synthesize a unit of biomass, is difficult to determine empirically [but see (*14*)]. Theoretical considerations suggest that the average energy required for biosynthesis of macromolecules from monomers is about 2400 J/g (*14*). This theoretical value of E_m gives an upper bound of $\gamma \sim 10$, the precise value depending on the additional energy expended on biosynthesis, metabolism, and excretion (*3*). For mammals and birds, γ averages about 3 and ranges from 1 to 9 depending on species, diet, and age (*3*, *14*, *18*). This result is consistent with values ranging from 0.8 to 7 for fish, birds, and mammals estimated from the OGM (*14*, *15*). We estimated from food assimilation that γ ranges from 0.6 to 5.3 with an average of 2.71 ± 1.18 (table S1), showing that, despite some variation, the empirical measurements are in agreement with the theoretical prediction. Values of f vary somewhat, depending on activity levels and behavior. The mean value of f estimated from food assimilation is 2.67 ± 0.61 (table S1), also in agreement with data for adult mammal and bird species (*14*).

When growth ceases, that is, $\mu = 1$ ($m = M$), Eq. 4 predicts that the food assimilation rate equals the total metabolic rate, which scales with mass, M. So, A is equal to $fB_0M^{3/4}$ across adults of different species. Data for ad libitum energy intake from food of 120 species of zoo mammals with body masses ranging from 0.025 kg to 3000 kg show $A = 7.07M^{0.75}$, supporting the prediction (*14*, *19*, *20*). Taking the average value of B_0 for resting metabolic rates of mammals, 3.92 W/kg$^{3/4}$ (*14*), gives $f \approx 1.8$. This is somewhat less than that expected for wild animals, which may reflect lower activity levels in captivity.

Our model predicts that growth rates of diverse animals should exhibit universal properties. The fraction of energy assimilation rate allocated to growth is the sum of S and B_{syn}. With Eq. 2 and the definition of γ, this fraction becomes $S + B_{\text{syn}} = (1+\gamma)B_{\text{rest,adult}}(\mu^{3/4} - \mu)$. If we normalize this quantity with respect to $(1+\gamma)B_{\text{rest, adult}}$, then all animal species, regardless of taxon or adult mass, should fall on the same parameterless universal curve, $\mu^{3/4} - \mu$. This further predicts that the maximum energy utilization rate for growth occurs when $d(\mu^{3/4} - \mu)/d\mu|_{\mu=\mu_0} = 0$, which gives $\mu_0 = (3/4)^4 = 0.316$. Equation 3 suggests a way to test these predictions. If we subtract the rate of metabolism for activity, B_{act}, and maintenance, B_{maint}, from the assimilation rate, A, the difference gives the rate of energy assimilation allocated to growth, $S + B_{\text{syn}}$. This quantity, normalized as above, is plotted as a function of the relative mass μ in Fig. 3A. The normalized assimilation rates for mammals and birds of widely varying body sizes and taxa show such universal properties, clustering closely around the predicted parameterless curve with a peak at ~0.316.

Additionally, the rate of energy allocation to growth must be proportional to the growth rate, dm/dt, so the universal curve and the value of $\mu_0 = (3/4)^4 = 0.316$ can be derived independently from the growth rate equation, Eq. 2, $dm/dt = (B_0/E_m)m^{3/4}[1 - (m/M)^{1/4}]$. This can be re-expressed as $(E_mM^{1/4}/B_0)d\mu/dt = \mu^{3/4} - \mu$. Data for normalized growth rates, $(E_mM^{1/4}/B_0)d\mu/dt$, for diverse mammals and birds measured independently from the above measurements of assimilation rate support this prediction (Fig. 3B). So, estimations from the rate of food assimilation and the rate of change in body mass independently predicted analogous universal curves with a maximum at a normalized body mass of ~0.316.

The predicted allometric scalings of metabolic energy allocation are summarized in Fig. 4A, which shows the rates of food assimilation and total, resting, and maintenance metabolism for two individuals of different adult size depicted by different colors. The figure illustrates the complete energy budget during growth, $A = B_{\text{maint}} + B_{\text{act}} + B_{\text{syn}} + S$, and allocation of energy at any given size is shown by the colored vertical lines. The assimilation rate, A, of a growing individual does not scale as a power law with mass, whereas its rates of total and resting metabolism, B_{tot} and B_{rest}, both scale as $m^{3/4}$ and its maintenance rate, $B_{\text{maint}} = B_m m$, scales linearly. In contrast, for adults of different sizes, rates of assimilation and total (dashed line) and resting (maintenance, solid black line) metabolism all scale as $M^{3/4}$. Across species of different adult masses, growth ceases when all resting metabolism is allocated to maintenance (*7*) so that $B_{\text{rest}} = B_{\text{maint}}$, as indicated in Fig. 4A (circles) representing two different adult masses, M_1 and M_2. Lastly, if otherwise identical individuals vary in energy allocated to activity, thereby having different values of B_{act} and B_{tot}, they must compensate by adjusting their assimilation rates, A, if they are to mature at the same adult mass, M.

One implication of the model is that when two individuals with the same B_0, f, and γ but different adult body masses, M_1 and M_2 ($M_1 > M_2$), have the same body mass, m, during growth, the assimilation rate of the one with the greater adult mass, M_1, must be larger than the one with the smaller adult mass, M_2, that is,

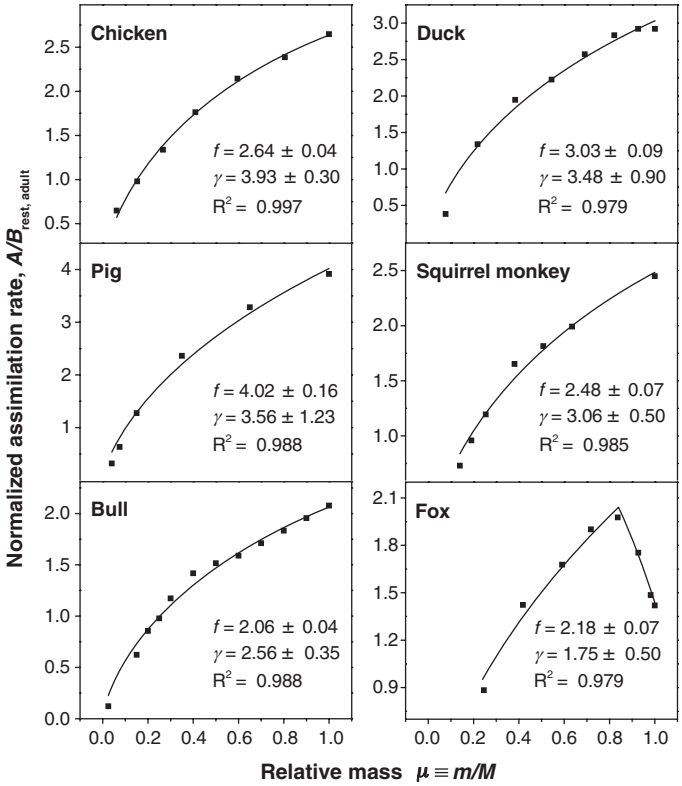

Fig. 2. Examples of normalized assimilation rate as a function of relative body mass for six mammals and birds (squares). The solid lines are fits of our model to these data with use of Eq. 4. (Parameters f and γ were estimated by using a nonlinear least squares regression method based on the Levenberg-Marquardt algorithm.) The majority of assimilation rate curves reported in the literature are monotonic, but a few, including curves for furbearers such as fox, are peaked relationships (*14*).

$A(m, M_1) - A(m, M_2) \propto (M_2^{-1/4} - M_1^{-1/4})m > 0$. To test this prediction, we plotted the assimilation rates of three pairs of closely related animals assumed to have the same B_0, f, and γ as a function of body mass m during growth. As illustrated in Fig. 4B, when members of each pair had the same body mass, m, during growth, the one with larger adult size (M) had a higher assimilation rate.

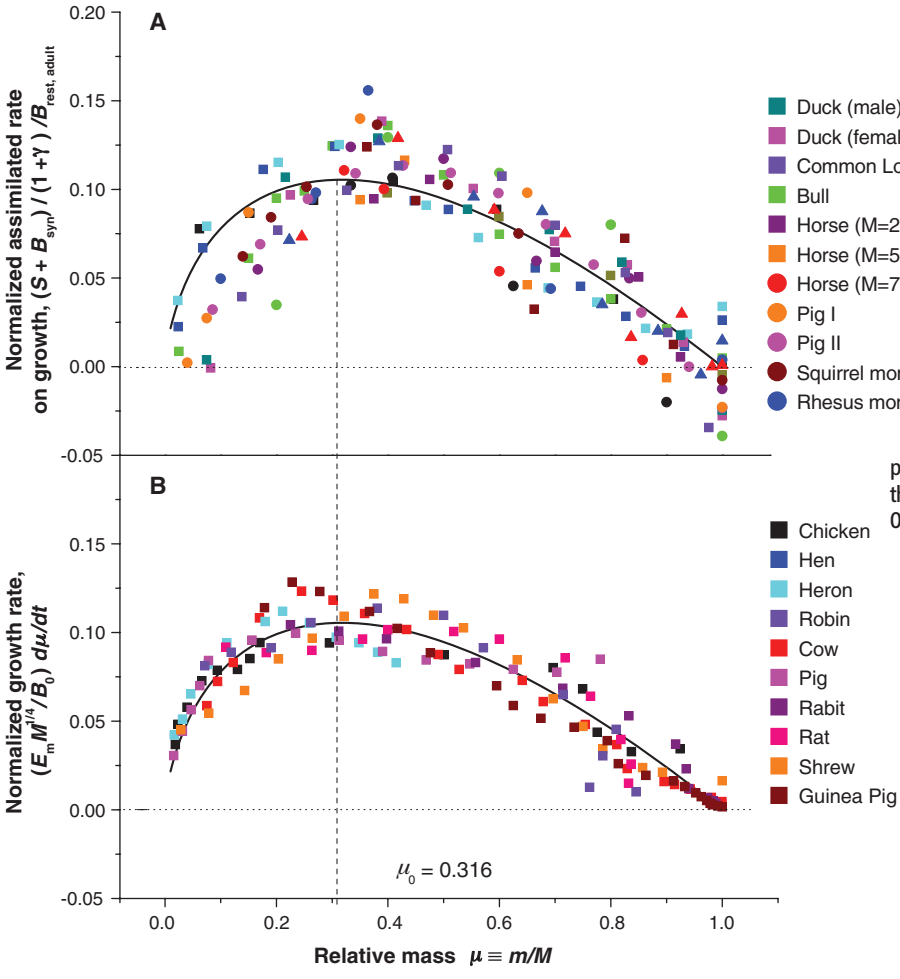

Fig. 3. Two growth curves that are universal in the sense that they have their bases in principles of energy allocation and are predicted to be independent of taxon and body size: (**A**) universal rate of assimilation of food for growth and (**B**) universal rate of change in body mass. The empirical estimates [colored symbols for different organisms, with assimilation and growth rates measured independently in different studies (*14*)] closely match the theoretical predictions (continuous curves that peak at 0.316).

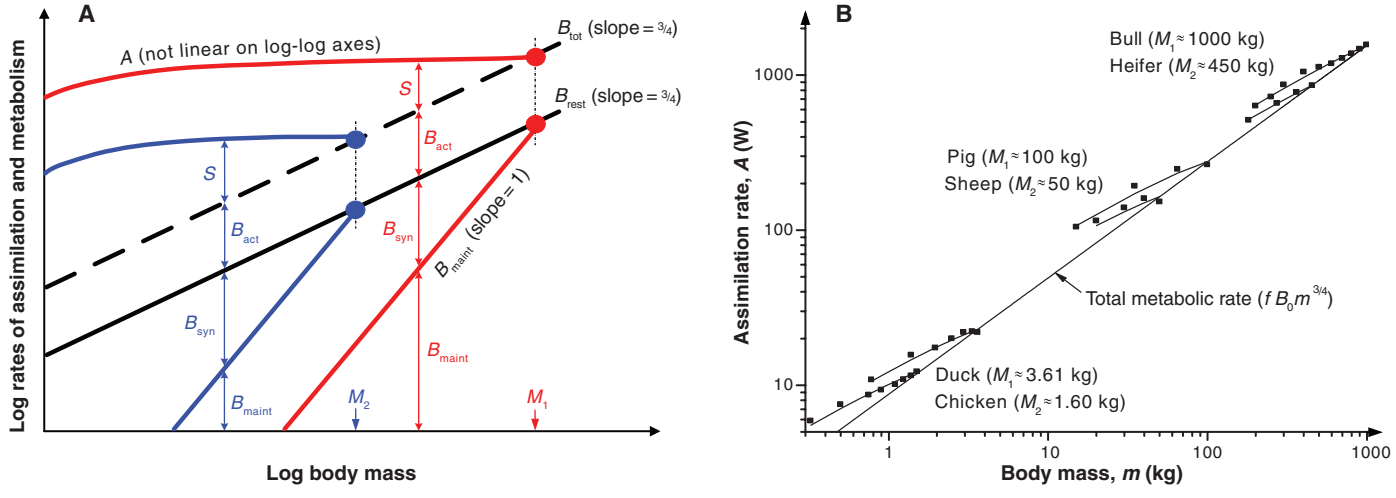

Fig. 4. (**A**) Schematic illustrating the allometric scalings of energy allocation during growth for two individual organisms (shown with different colors) of different adult sizes, M_1 and M_2. For each individual, the colored vertical lines illustrate how, at any given body mass during ontogeny, the rates of energy allocated to maintenance (B_{maint}), biosynthesis (B_{syn}), activity (B_{act}), and storage (S) sum to equal the rate of assimilation, A. The scalings across individuals of two different body sizes are shown as dashed and solid black lines for total and resting metabolic rates, respectively, with the colored dots corresponding to these rates at the adult sizes, M_1 and M_2. (**B**) Assimilation rate as function of body mass for three pairs of mammals or birds. To facilitate comparison, we assumed that $f = 2.67$ for all animals.

Our quantitative, predictive model for the energy budget of an individual during growth differs from phenomenological models that fit curves to data. It also differs from dynamic energy budget theory (DEB), which assumes a 2/3 power scaling of food assimilation rate during ontogeny, on the basis that energy uptake is limited by absorptive surface area, which scales like any simple geometric surface (*4*). By contrast, our model predicts that food assimilation rate cannot have a simple power-law scaling relation with body mass during ontogeny. Furthermore, DEB assumes that food assimilation rate is supply-limited, whereas our model views assimilation rate as arising from the developing organism matching food supply to metabolic energy demand. Our model provides a point of departure for addressing pathological cases of imbalance between supply and demand such as starvation or overeating. It captures the salient features of energy acquisition and allocation during ontogenetic development and quantitatively predicts universal assimilation and growth rate curves in agreement with data for mammals and birds. How well it captures the fundamental features of growth in other organisms, such as ectothermic vertebrates, insects, aquatic invertebrates, plants, and unicellular algae and protists, remains to be seen.

References and Notes

1. M. Kleiber, *The Fire of Life: An Introduction to Animal Energetics* (Wiley, New York, 1961).
2. S. Brody, *Bioenergetics and Growth* (Hafner, Darien, CT, 1964).
3. P. C. Withers, *Comparative Animal Physiology* (Saunders College/Harcourt College, Fort Worth, TX, 1992).
4. S. A. L. M. Kooijman, *Dynamic Energy and Mass Budgets in Biological Systems* (Cambridge Univ. Press, Cambridge, 2000).
5. R. E. Ricklefs, *Funct. Ecol.* **17**, 384 (2003).
6. A. M. Makarieva, V. G. Gorshkov, B. L. Li, *Ecol. Model.* **176**, 15 (2004).
7. G. B. West, J. H. Brown, B. J. Enquist, *Nature* **413**, 628 (2001).
8. M. Jobling, *J. Fish Biol.* **23**, 549 (1983).
9. M. D. McCue, *Comp. Biochem. Physiol. A* **144**, 381 (2006).
10. A. Ashworth, *Nature* **223**, 407 (1969).
11. I. Krieger, *Am. J. Clin. Nutr.* **31**, 764 (1978).
12. K. L. Blaxter, *Energy Metabolism in Animals and Man* (Cambridge Univ. Press, Cambridge, 1989).
13. K. A. Nagy, I. A. Girard, T. K. Brown, *Annu. Rev. Nutr.* **19**, 247 (1999).
14. Materials and methods are available as supporting material on *Science* Online.
15. M. E. Moses *et al.*, *Am. Nat.* **171**, 632 (2008).
16. K. W. Cummins, J. C. Wuycheck, *Mitt. Int. Ver. Theor. Angew. Limnol.* **18**, 1 (1971).
17. C. T. Robbins, *Wildlife Feeding and Nutrition* (Academic Press, New York, 1983).
18. R. E. Ricklefs, in *Avian Energetics*, R. A. Paynter Jr., Ed. (Nuttall Ornithological Club Publication Number 15, Cambridge, MA, 1974).
19. E. Evans, D. S. Miller, *Proc. Nutr. Soc.* **27**, 121 (1968).
20. J. K. Kirkwood, *J. Nutr.* **121** (suppl. 11), 29 (1991).

21. Supported by NIH grants P20 RR-018754 (for M.E.M.) and DK36263 (for W.H.W.) and by NSF grants DEB-0083422 and CCF0621900 (for J.H.B.) and PHY 0706174 and PHY 0202180 (for G.B.W.) G.B.W. also acknowledges the Thaw Charitable Trust for its support.

Supporting Online Material

www.sciencemag.org/cgi/content/full/322/5902/736/DC1
Materials and Methods
Tables S1 to S7
References and Notes

25 June 2008; accepted 19 September 2008
10.1126/science.1162302

Experimental Evidence for Spatial Self-Organization and Its Emergent Effects in Mussel Bed Ecosystems

Johan van de Koppel,[1]* Joanna C. Gascoigne,[2] Guy Theraulaz,[3] Max Rietkerk,[4] Wolf M. Mooij,[5] Peter M. J. Herman[1]

Spatial self-organization is the main theoretical explanation for the global occurrence of regular or otherwise coherent spatial patterns in ecosystems. Using mussel beds as a model ecosystem, we provide an experimental demonstration of spatial self-organization. Under homogeneous laboratory conditions, mussels developed regular patterns, similar to those in the field. An individual-based model derived from our experiments showed that interactions between individuals explained the observed patterns. Furthermore, a field study showed that pattern formation affected ecosystem-level processes in terms of improved growth and resistance to wave action. Our results imply that spatial self-organization is an important determinant of the structure and functioning of ecosystems, and it needs to be considered in their conservation.

Self-organized spatial patterns in ecological communities have been observed in arid ecosystems (*1*–*3*), peat lands (*4*), tidal wetlands (*5*), mussel beds (*6*), and rocky shores (*7*–*9*). These patterns are thought to result from local, nonlinear interactions between organisms or between organisms and the environment, developing even on completely homogeneous substrates. Models predicted that self-organized patterns can affect ecosystem-level processes, for instance, by improving resilience to perturbation, resistance to environmental change, and primary or secondary production (*3*, *6*). Most studies of self-organization in ecological systems combine observational studies with mathematical modeling (*2*, *10*) or experimentally test the mechanisms that underlie the self-organization process (*11*). Experimental demonstrations of self-organization—as have been accumulated for physical, chemical (*12*, *13*), sociobiological (*14*), and microbial systems (*15*, *16*)—are rare for ecological systems (*17*, *18*).

We investigated the origin of regular patterns in beds of the blue mussel *Mytilus edulis* (in the Menai Strait near Bangor, UK) on intertidal flats under wind-sheltered conditions (*19*). *M. edulis* is a filter-feeding animal exploiting algal plankton and detritus in the water column. Patterns consist of regularly spaced clusters of 5 to 10 cm in width that form a coherent, labyrinth-like pattern (Fig. 1A). In areas where mussel densities are lower, clusters are more isolated (Fig. 1B), whereas beds are near-homogeneous in very dense areas. Point pattern analysis based on Ripley's K (*19*) revealed clear, regularly spaced mussel clusters of ~3 to 5 cm across at ~10 cm distance from each other (fig. S1). Despite an order of magnitude difference in mussel biomass at the scale of meters, we found no significant difference in within-cluster biomass (fig. S2), suggesting that mussels self-organize to a certain local, within-cluster density, possibly to minimize predation or dislodgement losses (*20*). This concurs with a number of mathematical studies pointing at the possibility of self-organized pattern formation in mussel beds (*6*–*8*) and experimental studies in other intertidal ecosystems (*18*, *21*). Because of their small spatial scale, fast temporal development, and easy manipulation and observation of individuals, mussel beds are particularly suited for experimental testing of self-organization principles.

We tested in the laboratory the hypothesis that the observed patterns are self-organized and hence would develop spontaneously from homogeneity. Mussels that were laid out evenly in laboratory mesocosms developed coherent non-random spatial patterns within a day. These patterns were statistically similar to the patterns observed in the field (Fig. 1, C and D; movie S1; and see fig. S3, A and B, for a statistical description). When mussel densities in the laboratory were decreased, the spatial pattern became more open and clumps became more isolated (Fig. 1, E and F; movie S2; and fig. S3, C to D), as was observed under natural conditions (fig.

[1]Spatial Ecology Department, the Netherlands Institute of Ecology (NIOO-KNAW), Post Office Box 140, 4400 AC Yerseke, Netherlands. [2]School of Ocean Sciences, University of Wales Bangor, Askew Street, Menai Bridge LL59 5AB, UK. [3]Centre de Recherches sur la Cognition Animale, CNRS UMR 5169, Universite Paul Sabatier 118, Route de Narbonne, 31062 Toulouse Cedex 04, France. [4]Department of Environmental Sciences, Copernicus Institute, Utrecht University, Post Office Box 80115, 3508 TC Utrecht, Netherlands. [5]Aquatic Food Webs Department, Netherlands Institute of Ecology, Rijksstraatweg 6, 3631 AC, Nieuwersluis, Netherlands.

*To whom correspondence should be addressed. E-mail: J.vandeKoppel@nioo.knaw.nl